CONF-801002--1

THERMAL-HYDRAULICS OF THE PBF/LOFT LEAD ROD LOSS-OF-COOLANT EXPERIMENTS

D. J. Varacalle, Jr., R. W. Garner, P. E. MacDonald, W. R. Cox[a]
EG&G Idaho, Inc.
P.O. Box 1625
Idaho Falls, Idaho 83401

ABSTRACT

Results of the four PBF/LOFT Lead Rod sequential blowdown tests conducted in the Power Burst Facility (PBF) are presented. The primary objective of the test series was to evaluate the extent of mechanical deformation that would be expected to occur to low pressure (0.1 MPa), light water reactor design fuel rods subjected to a series of nuclear blowdown tests, and to determine if subjecting deformed fuel rods to subsequent testing would result in rod failure. The extent of mechanical deformation (buckling, collapse, or waisting of the cladding) was evaluated by comparison of cladding temperature versus system pressure response with out-of-pile experimental data, and by posttest visual examinations and cladding diametral measurements. Tests LLR-3, LLR-5, LLR-4, and LLR-4A were performed at system conditions of 595 K coolant inlet temperature, 15.5 MPa system pressure, and 41, 46, 57 and 56 kW/m test rod peak linear powers, respectively, at initiation of blowdown. Cladding temperatures during the tests ranged from 870 to 1260 K. Test LLR-4 was the first test of the series during which observed cladding surface temperatures were sufficiently high (ranging from 1060 to 1170 K) to result in maximum cladding deformation. Test LLR-4A was performed after Test LLR-4 for the purpose of subjecting the deformed rods to subsequent power histories and blowdown conditions. None of the deformed rods failed during Test LLR-4A. The RELAP4 pretest calculations of coolant behavior agreed well with the measured coolant behavior; however, calculated cladding surface temperatures were overpredicted at the thermocouple locations. The PBF/LOFT Lead Rod Test

---

a. Presently employed by Rockwell International, Sulphur Springs, Texas.

Series demonstrated that low pressure, light water reactor design fuel rods can withstand multiple blowdown transients at power densities as high as 57 kW/m without failure. This information is directly applicable to the LOFT Power Ascension Test Series and, in general, to nuclear reactor safety.

INTRODUCTION

Results from the PBF/LOFT Lead Rod (LLR) nuclear blowdown tests are presented. The PBF/LLR test series was conducted by the Thermal Fuels Behavior Program of EG&G Idaho, Inc., in the Power Burst Facility (PBF) reactor at the U. S. Department of Energy's Idaho National Engineering Laboratory (INEL) near Idaho Falls, Idaho, for the U. S. Nuclear Regulatory Commission under funding provided by the Japanese Atomic Energy Research Institute (JAERI). The primary objectives of the PBF/LLR Test Program were: (a) to intentionally subject low pressure (0.1 MPa), light water reactor design fuel rods to loss-of-coolant accident (LOCA) conditions resulting in waisting (collapse into pellet-to-pellet gaps) of the cladding, and (b) to evaluate the effects of pellet-cladding interaction (PCI) during subsequent preconditioning power transients with deformed fuel rods. The results of the PBF/LLR tests have direct application to evaluating the extent of fuel rod deformation that would be expected to occur during the LOFT LOCA Power Ascension Test Series,[1] and the consequences of continued operation of the LOFT core with deformed fuel rods. In addition, the experimental data can be used in evaluating computer codes that are used to predict reactor system and fuel rod behavior during LOCA conditions.

The PBF/LLR Test Series originally consisted of three tests, designated LLR-3, LLR-5, and LLR-4, that were designed and performed to simulate the behavior of LOFT design fuel rods during the LOFT Power Ascension Test Series Tests L2-3, L2-5, and L2-4, respectively. Each test was performed with four, identical, separately shrouded LOFT design fuel rods. Test conditions for Tests LLR-3, LLR-5, and LLR-4 were approximately 595 K inlet coolant temperature, 15.5 MPa system pressure, and 41, 46 and 57 kW/m peak linear power, respectively, in the test rods. Test conduct included several hours of steady state operation at various power levels to precondition the fuel, at least two hours steady state operation at the desired test power level to

build up approximately 80% of the maximum possible decay heat in the test rods, followed by system blowdown and subsequent reactor scram. During the preconditioning phase, changes in power levels were accomplished at ramp rates of 4.92 kW/m/h (Tests LLR-3 and LLR-5) and 6.56 kW/m/h (Test LLR-4). System thermal-hydraulic parameters and fuel rod pressures, temperatures, and coolant flow conditions were monitored throughout the various test phases.

Prior to the performance of the PBF/LLR tests, and any of the LOFT tests, it was expected that Test LLR-5 would result in waisting of the cladding and that Test LLR-4 would be performed to provide the desired information on the effects of pellet-cladding interaction during subsequent testing with deformed fuel rods. However, fuel rod cladding temperatures attained during Tests LLR-3 and LLR-5 were somewhat lower than anticipated, and maximum fuel rod cladding deformation may not have occurred until the highest power test (Test LLR-4) was performed. Since a major objective of the LLR tests was to investigate the effect of cladding collapse and waisting on rod behavior during subsequent power ramps and blowdown transients, Test LLR-4A was added to the test program. This experiment was performed at the same test conditions as Test LLR-4.

Cladding temperatures during the tests ranged from 870 to 1260 K. The RELAP4 pretest calculations of coolant behavior agreed well with the measured coolant behavior; however, calculated cladding surface temperatures were overpredicted because the time to critical heat flux (CHF)[a] was calculated to occur sooner than it was measured at the thermocouple locations.

TEST DESIGN AND CONDUCT

Each test was performed with four identical, unpressurized, LOFT-type fuel rods, each surrounded by an individual circular flow shroud and symmetrically positioned in the in-pile tube (IPT) test space of the PBF

---

a. Preliminary results of tests recently performed for the specific purpose of evaluating the effect of cladding external surface thermocouples on fuel rod response during blowdown transients indicate that the cladding thermocouples may indeed delay the onset of DNB, resulting in lower measured cladding surface temperatures. Further evaluation of these test results may influence the design and performance of future LOCA type tests.

reactor which provides a test environment with typical PWR coolant pressures, temperatures, and flow rates. Test performance involved a preconditioning phase, a blowdown phase, and a reflood phase typical of the planned LOFT tests.

The fuel rods were of the type used in a typical PWR 15 x 15 rod array, except for the active length, which was 0.91 m (a PWR 15 x 15 bundle fuel rod is 3.66 m long). The plenum volume was scaled in proportion to the active fuel length. The seven fuel rods used in the test series were initially prepressurized with helium to 0.1 MPa.

Steady state test conduct was initiated with the preconditioning phase for each test which consisted of (a) several slow power ramps from low powers to successively higher powers to provide data for calibration of the test rods with the PBF core power, and (b) steady state operation for two hours at a peak linear power consistent with the LOFT counterpart test to provide approximately 80% maximum decay heat buildup. Typical PWR system conditions prior to blowdown were approximately 595 to 600 K inlet coolant temperature to the test rods, coolant flow rates from 0.584 to 0.80 l/s (depending on rod power) through each flow shroud, and a system pressure of 15.5 MPa. The measured initial conditions for the LLR tests prior to blowdown are shown in Table I.

TABLE I MEASURED INITIAL CONDITIONS FOR THE LLR TESTS PRIOR TO BLOWDOWN

Test	Maximum Rod Power (kW/m)	System Pressure (MPa)	Inlet Temperature (K)	Average Core Differential Temperature	Shroud Flow (l/s)	Fission[a] Heat (s)
LLR-3	40.5	15.67	595.0	11.1	0.58	0.0
LLR-5	47.4	15.5	598.0	10.5	0.60	2.0
LLR-4	56.6	15.6	600.0	10.1	0.80	2.6
LLR-4A	55.6	15.5	600.0	11.5	0.78	2.85

a. Fission heat refers to the duration following initiation of blowdown that the PBF core power was maintained in an effort to provide higher cladding temperatures during blowdown.

Figure 1 illustrates the PBF in-pile tube (IPT) and blowdown system. Figure 2 presents an illustration of a test fuel rod within a circular shroud, and the associated instrumentation.

Transient test operation was initiated with isolation of the IPT and experimental hardware from the PBF primary coolant system, and a simultaneous system blowdown. Blowdown commenced with the opening of the two high speed (~100 ms) blowdown valves, shown in Figure 1 in the cold leg of the coolant loop, to simulate a 200% double-ended cold leg break LOCA. Approximately 3.75 seconds after initiation of blowdown, the large cold leg blowdown valve was closed until 22 seconds, when it was reopened. This valve sequencing was necessary to match the LOFT L2 Test Series predicted depressurization rates. Valve operation was controlled by a time sequential programmer. The break planes were formed by converging-diverging nozzles with a cylindrial throat section having equal length and diameter. The throats were sized to control the blowdown flow and depressurization rates. The coolant ejected from the IPT was collected in the system blowdown tank. Reflood was performed by injecting coolant from a quench tank directly into the IPT. After reflood, additional posttest quench cooling was provided to completely flood the fuel rods and terminate the test.

Fuel rod cladding temperatures were maximized by the use of continued fission heat after initiation of blowdown. Table I presents the time after blowdown at which the PBF reactor was scrammed for each test. The PBF reactor power was essentially maintained at the steady state power level for these time periods after initiation of blowdown.

The fuel rod instrumentation consisted of cladding surface thermocouples, fuel centerline thermocouples, linear variable differential transformers (LVDT) for measurement of axial elongation, plenum pressure transducers, and plenum thermocouples. The test train instrumentation consisted of turbine flowmeters located at each end of the fuel rod flow shrouds, coolant temperature thermocouples, coolant pressure transducers, and thermocouples on the outer surface of the fuel rod flow shroud.

Instrumentation spool pieces were installed in the cold leg inlet and cold and hot leg blowdown lines for determination of the inlet and blowdown coolant conditions. Each spool contained instrumentation for measurement of coolant temperature, pressure, volumetric flow rate, and momentum flux. The spools in the blowdown piping also contained a three-beam gamma densitometer to determine coolant density.

CALCULATIONAL TECHNIQUE

The RELAP4/MOD6 computer code[2,a] was used for pre- and posttest calculations of coolant thermal-hydraulic response and fuel rod thermal behavior for the LLR tests. RELAP4 is a code that can be used to predict the transient behavior of water cooled nuclear reactors (or simulators) subjected to postulated accidents such as those resulting from a LOCA. It is a comprehensive program that predicts the interrelated effects of coolant thermal-hydraulics, system heat transfer, core neutronics, and system component interactions. The code solves the governing conservation equations for mass, momentum, and energy using homogeneous flow theory and thermal-equilibrium conditions. The program requires input for the geometry of the system, including fluid volumes, initial flows, pressure and temperature distributions, power generation, and material properties.

The RELAP4/MOD6 model is shown in Figure 3, and the modeling options chosen for these calculations are listed in Table II.

To accurately predict the thermal response of a nuclear fuel rod during a PBF loss-of-coolant experiment (LOCE), the shroud thermal hydraulics must be accurately calculated. However, it was difficult to predict the shroud thermal-hydraulic behavior during an earlier LOC-11[3] series of tests. To control the thermal-hydraulics in the PBF IPT, several modifications to the LOC-11 test train were required, as shown in Figure 1a. These modifications included check valves located at the outlet of the fuel rod flow shrouds to

---

a. RELAP4/MOD6, Update 4, Version III, Idaho National Engineering Laboratory Configuration Control Number H00441IB.

TABLE II RELAP4 MODEL OPTIONS

1. The Henry-Fauske and homogeneous equilibrium subcooled and saturated break-flow models with multipliers of 1.0.
2. The MOD6 best-estimate blowdown heat transfer package, which includes:
   a. Tong's W-3 correlation for subcooled CHF
   b. the Hsu-Beckner modified W-3 correlation for saturated high-flow CHF
   c. the modified Zuber correlation for saturated low-flow CHF
   d. the modified Condie-Bengston transition boiling heat transfer correlation
   e. the Condie-Bengston III film boiling correlation
   f. natural convection and radiation heat transfer to superheated steam.
3. The RELAP4/MOD6 default model for slip at all vertical junctions.
4. The Ross and Stoute pellet-to-cladding gap conductance and the Cathcart-Pawel zircaloy metal-water reaction models.
5. A radial pin power profile and radiation heat transfer from fuel rod to shroud models (not available in the standard RELAP4/MOD6 version).

prevent coolant fallback from the upper plenum, a controlled bypass from the downcomer to the upper plenum to control the upper plenum flow path, relatively massive filler pieces located in the upper plenum and downcomer to more closely model a PWR ratio of core coolant to the coolant in these areas, and a cold leg blowdown to control the differential pressure from spool to spool.

TEST RESULTS

The fuel rod cladding deformation that may occur as a result of a rapid system depressurization from a high power condition has been investigated out-of-pile by Olsen.[4] From these studies, criteria were developed for evaluating the occurrences of cladding deformation in the form of (a) two-point buckling, (b) uniform circumferential cladding collapse, or (c) waisting, based on the cladding temperature and system pressure response during blowdown.

The LLR rod cladding temperature responses and system pressure responses were evaluated to provide information on the mechanical deformation of the cladding and were compared with the related data published by Olsen.

Mechanical deformation of the low pressure fuel rods occurred during the early part of the blowdown when cladding temperatures were near their maximum values and the system pressure was still relatively high. During this time, the system thermal-hydraulic response was similar for all the PBF/LLR tests since the initial conditions at the time of blowdown were essentially the same.

System Thermal-Hydraulic Response During Blowdown

Since in-core thermal-hydraulic measurements are not sufficient to directly determine the fuel rod boundary conditions, the RELAP4/MOD6 code was used to confirm the expected system thermal-hydraulic behavior and coolant behavior in each fuel rod flow shroud. The variables that affect system response, and thus fuel rod behavior, include coolant pressure, density, temperature, and flow. The system pressure, in conjunction with the fuel rod internal pressure and cladding temperature, provides the driving forces that govern fuel rod cladding deformation. The pressure distribution within the system provides the driving potential for coolant flow through the fuel rod flow shrouds. The coolant temperature and density define the fluid state of the mass flow leaving the system. The system break flow, and hence the fuel rod shroud mass flow rate, directly determines the cladding surface heat flux, the cladding temperature, the system depressurization, and the coolant mass ejection.

In the following sections the coolant break flow rate, system depressurization, fuel rod shroud volumetric flow, coolant temperature, and coolant density are evaluated and discussed. The data are also compared with pretest calculations, which were performed with RELAP4.

The coolant thermal-hydraulic behavior during the PBF/LLR tests was similar. For this reason, only results from Test LLR-5 are described in this paper as being typical of the thermal-hydraulics observed during all the tests. Fuel rod thermal response for all the tests is discussed in a subsequent subsection.

System Depressurization

Figure 4 presents the measured and calculated system depressurization in the cold leg spool piece during Test LLR-5. The RELAP4 pretest predictions also represent the LOFT required depressurization for this test. A steady state pressure of approximately 15.5 MPa was achieved prior to blowdown. With the initiation of the cold leg blowdown transient, the system depressurized to the vapor pressure of the coolant in approximately 50 ms. The coolant pressure decreased during this subcooled depressurization from the initial value to the saturation pressure (10.7 MPa), corresponding to a system mixing cup saturation temperature of 589 K. As shown in Figure 4, the subcooled and saturated portions of the blowdown matched the desired depressurization extremely well. After the system pressure dropped to the level of the coolant vapor pressure, steam voids were formed. The sonic velocity was drastically reduced at this point, the pressure waves propagating through the system were damped out, and choking at the break point occurred. After this initial decrease to saturation conditions, the data is slightly lower than the LOFT required depressurization (as calculated by RELAP4) for the majority of the saturated blowdown. The slight increase in measured system pressure at 3.75 s is attributed to closing the large cold leg blowdown valve. The code calculations follow this trend extremely closely. From this point, the data indicate a less rapid depressurization than the code calculations until 22 s, at which time the two plots coincide. This difference is attributed to the difference in the calculation of the break flow rate. The effect of reopening the large cold leg blowdown valve is evidenced at this time as the slope of the depressurization data increases for the remainder of the transient. The changes in system pressure during the opening and closing of the large cold leg blowdown valve corresponds closely to observed measurement spikes in break mass flow discussed in a subsequent section.

Figure 5 compares the predicted (pretest) and measured pressure differential between the hot and cold leg blowdown spools (which is representative of the differential between the IPT upper and lower plenums, respectively). At steady state, the cold leg spool pressure was approximately 0.18 MPa higher than the hot leg spool pressure. When blowdown was initiated, the pressure differential was reversed, resulting in a 0.55 MPa differential

from the upper plenum to the lower plenum. This rapidly closed the check valves on the top of each flow shroud, resulting in rapid coolant voiding and a saturated steam environment for each fuel rod. At 3.75 s into the transient the large cold leg blowdown valve was closed, resulting in a decrease in the pressure differential to 0.05 MPa, at which value it remained until 22 s. At this time the large cold leg blowdown valve was reopened, causing the pronounced increase in the pressure differential. The comparison between the RELAP4 predictions and the experimental data shows good agreement, indicating the code-calculated system resistances are reasonable.

System Coolant Temperatures

With the initiation of the blowdown transient, the system subcooled depressurization reduced the coolant temperature at the various locales in the IPT and piping legs to saturation conditions. Figure 6 shows a comparison between the pretest RELAP4 calculation and the coolant temperature measurement in the cold leg spool piece for Test LLR-5. The fluid temperature gradually decreases with the system pressure presented in Figure 2, following a saturation line decrease until 22 seconds. The RELAP4 predictions are in reasonable agreement with the measurements during this period of time, slightly overpredicting the data for the first 17 seconds. At 23.5 seconds, the data indicate a superheated environment in the spool piece.

System Coolant Density

The PBF/LLR experiments measured coolant density in the hot and cold leg spool pieces with three-beam gamma densitometers. Figure 7 presents the predicted (pretest) and average measured coolant density in the cold leg spool piece as a function of time. The RELAP4 prediction generally compares well with the experimental data. However, the measured density is higher than the calculated density during the first second of the transient and lower than the calculated density from about 2 to 4 seconds. This is attributed to measurement response time errors. Beyond approximately 12.5 seconds, the experimental data exhibits a slightly higher density than the predictions.

System Flow

Because of the IPT differential pressure reversal, shown in Figure 5, the check valves on top of the flow shrouds shut nearly instantaneously upon initiation of the blowdown. This forced the two-phase coolant in the bypass region and above the lower support plate into the upper plenum and out the controlled bypass flow path to the cold leg. Figure 8 presents the measured and predicted controlled bypass volumetric flow rate. Approximately 33% of the total system volume passes through the controlled bypass. As is evident, RELAP4 significantly underpredicted the volumetric flow through this flow path. Since the differential pressure across the spool pieces was matched relatively well, the fluid state calculated by RELAP4 must be in error. The heat transfer in this region was complicated due to the substantial metal mass in the upper plenum, and the code was apparently not able to predict the correct phase separation in the bypass and upper plenum volumes. A much higher quality must have existed in these two regions than was predicted by RELAP4.

The mass flow leaving the LOCA blowdown system in transit to the blowdown tank during a LOCE is a difficult variable to calculate. However, the use of specially designed converging-diverging nozzles with cylindrical throat sections of length equal to the diameters, optimized the capability to calculate break flow. A combination of the Henry-Fauske (subcooled flow) and homogeneous equilibrium model (saturated flow) correlations for critical flow were used in the RELAP4 model to describe the flow at the throats of the blowdown nozzles. In studying the results of previous PBF-LOCA tests, it was determined that a break flow multiplier[a] of 1.0 (RELAP4 default valves) should be used to obtain the best agreement between the RELAP4 calculations and the data.

The volumetric flow rate at the cold leg blowdown spool is shown in Figure 9 along with the RELAP4 pretest prediction. The initial flow spike to

a. The multiplier is a constant selected to optimize comparison between the code prediction and experimental data for various throat diameters.

60 l/s occurred when the cold leg blowdown valves, located between the measurement spool and the blowdown nozzles, were first opened. A slug of fluid filled the piping between the nozzle and valve and immediately resulted in choked flow at the break plane, as the reduced pressure at the nozzle throat resulted in rapid steam formation. As the system pressure dropped 4.8 MPa in 50 ms at the cold leg spool, the driving potential for flow out the break was reduced, resulting in a reduction in volumetric flow from 60 to 40 l/s within 0.5 s. The volumetric flow again increased to 60 l/s during the interval from 1.0 to 3.75 s. This is attributed to an increase in coolant quality from 0.0 to 0.28 during this time period, with the resulting decrease in density and increase in void fraction to approximately 85%. The severe drop-off in flow at 3.75 s is attributed to closing the large cold leg blowdown valve. The flow then gradually increased due to the constantly increasing quality until 22 s, when the valve was reopened, resulting in high volumetric flows for the remainder of the blowdown transient. The RELAP4 code predicted the cold leg volumetric flow during both the subcooled and saturated portions of the blowdown extremely well. This indicates that the code predicted the correct volume of two-phase mixture leaving the system.

The cold leg spool average mass flow rate for Test LLR-5 is shown in Figure 10 along with the corresponding RELAP4 calculations. The mass flow was determined from the average coolant density and coolant volumetric flow rate by combining information from the gamma densitometer and turbine meter. The overall agreement between the predicted and measured mass flow rates is favorable, except during the initial subcooled flow spike and for the period from 2.5 to 4.0 s. The mass flow data for the first second of the transient was higher than predicted and probably in error due to the problems in measuring the cold leg coolant density discussed above. From 2.5 to 4.0 s the measured density was lower than predicted, resulting in a higher predicted mass flow. Beyond 5 s, the predicted mass flow rate is slightly lower than the measured value. The effect of the blowdown valve sequencing is evident again at 3.75 and 22 s, as the mass flow decreases sharply, then increases slightly with the closing and subsequent reopening of the large cold leg blowdown valve.

Fuel Rod Shroud Flow

The steady state inlet volumetric flow to the IPT for Test LLR-5 was approximately 9.35 l/s, as measured at the inlet spool piece. Approximately 6.7 l/s passed through the controlled bypass, with the remaining flow passing through the four flow shrouds (∿2.4 l/s), and a small amount of flow (∿.25 l/s) attributed to various leakages throughout the test train. The warmup line from the cold leg to the hot leg was closed until just prior to blowdown.

The flow in the fuel rod shrouds during the blowdown is primarily controlled by depressurization of the lower plenum. Because of the unique configuration of the PBF/LLR test train, the upper and lower plenums depressurized independently. Upon initiation of blowdown, the check valves located on the top of each flow shroud shut nearly instanteously as the IPT lower to upper plenum differental pressure reversed. This completely isolated the coolant in the flow shrouds from an upper plenum or volumetric bypass flow path, and the direction of shroud flow remained negative throughout the blowdown transient.

The shroud inlet and outlet volumetric flow rates for Rod 312-1 during Test LLR-5 are shown in Figures 11 and 12, respectively, along with the corresponding RELAP4 pretest predictions. For the most part, both the data and predictions for the other test rods for all the other LLR tests follow the trends set forth by Rod 312-1.

Upon initiation of blowdown, flashing first occurred in the fuel rod flow shrouds where the highest enthalpy fluid was located. The upper turbine volumetric flow rate decreased sharply from the initial steady state upflow of 0.58 l/s, and reversed to a value of -0.25 l/s. This small, initial, negative flow spike lasted only momentarily as the flow immediately stagnated in the upper portion of the flow shrouds. The lower turbine meter was saturated at -1.5 l/s, its mechanical limit, upon initiation at blowdown. As flow choked at the blowdown nozzles, the flow in the lower turbine decreased to -0.8 l/s. Beyond this point the data indicate a relatively significiant amount of volumetric flow until the large cold leg blowdown valve was closed at 3.75 s.

At this point, the flow decreased sharply, then gradually stagnated for the remainder of the transient until 22 seconds, when the reopening of the blowdown valve generated flows comparable to those during the first 5 seconds.

As shown in Figure 11, the RELAP4 calculations do not predict the small, initial, negative flow spike in the upper turbine, but follow the measured data rather closely after this time period. The magnitude and duration of the initial negative flow spike was calculated well at the lower flowmeter, however. After the initial flow spike, the agreement between the lower volumetric flow rate and the calculation was not as good for the first 4 seconds. This is probably associated with incorrect modeling of phase separation and steam superheating in the shrouds. The magnitude of volumetric flow was undercalculated by as much as 0.2 l/s. Past this point the calculations follow the measured trends extremely closely.

Accurate calculation of the magnitude of the volumetric flow in the flow shrouds was complicated because of code modeling assumptions. The RELAP4 code is based on the assumption of homogeneous flow with thermodynamic equlibrium. In actuality, the conditions within the shrouds are nonhomogeneous and are not in thermodynamic equilibrium. Also, small differences between the actual and calculated coolant density will result in large differences in the volumetric flow rate. An indication of potential differences in density was suggested by the differences between the calculated and measured onset of superheated vapor in the shroud, as discussed in a subsequent session. Slip between the liquid and vapor phases (i.e., different velocities) was included in the RELAP4 model for the core vertical junctions by using the code default correlation. This correlation is solely a function of void fraction and directly affects the calculation of the energy equation, which in turn directly affects the fuel rod surface heat transfer. One final factor not accurately considered in the calculation of the local coolant density is the mixing of the phases by the top hat orifices located at the entrance and exit of each flow shroud.

The inability of the RELAP4 code to predict the time to CHF, discussed in a subsequent section for the LLR tests, is directly relatable to the prediction of density and the corresponding flow patterns in the shrouds.

The flow patterns observed in vertical co-current flow, as described by Collier,[5] include bubbly, slug, annular, churn, and wispy-annular flow. The presence of a heat flux through the channel wall alters these flow patterns from that which would have occurred in a long unheated channel at the same flow conditions. Since the LLR shroud flow patterns are further complicated by the annular flow area resulting from the shroud/fuel rod geometry and the presence of the fuel rod and channel wall heat fluxes, the problem of estimating the flow patterns is complicated. Hewitt[6] and co-workers have constructed the flow pattern map shown in Figure 13 from their observations of high pressure steam-water flow in small-diameter (1 to 3 cm) heated vertical tubes. The axes represent the superfical momentum fluxes of the liquid ($\rho_f j_f^2$) and vapor phases respectively. These momentum fluxes can also be expressed in terms of the mass velocity (G) and the quality (X).

$$\rho_f j_f^2 = \frac{[G(1-X)]^2}{\rho_f} \qquad \rho_g j_g^2 = \frac{(GX)^2}{\rho_g} \tag{1}$$

If the density in the shrouds is assumed to be slightly higher than that predicted by the RELAP4 pretest calculation, the flow pattern overlaid on Hewitt's map (Figure 13) is obtained. The flow map indicates that an annular flow regime is maintained for the first 6.5 s of the transient, when superheated steam conditions are then attained. This suggests the formation of a high velocity vapor core with a liquid film around the periphery of the shroud and fuel rod. Since the fuel rods achieved their maximum temperatures in the time period of 1.5 to 6 seconds, vapor that is formed at preferred positions on the surface of the rods, detaches with the high velocity steam flow intermittently. With the production of more vapor, the bubble population increases with length and coalescence takes place as CHF is attained and propagated up the rod. The flow shroud, on the other hand, probably maintained a liquid film until well after 6.5 s to maintain the volumetric flows shown in Figure 12.

Fuel Rod Shroud Coolant Temperature

As blowdown was initiated, the coolant temperatures within the flow shrouds immediately attained saturation conditions. Local qualities continued to rise during the first several seconds of the transient until they reached unity. The temperatures at these points then increased significantly above the saturation temperature. This superheating was attributed to the energy transfer by convection and radiation from the fuel rods and flow shrouds.

The coolant temperatures within the shroud of Rod 345-1 at several axial elevations are shown in Figure 14. The initial steady state temperature gradient of approximately 10 K across the flow shroud from inlet to outlet was due to the energy transfer from the fuel rods to the coolant. With the initiation of blowdown, the coolant temperatures remained at saturation and decreased as the system rod pressure decreased until 6.5 to 7 s. At this point, the three thermocouples at the fuel rod midplane and the thermocouple at the shroud inlet indicated a superheated steam environment which was maintained throughout the remainder of the transient. The coolant thermocouple at the shroud outlet followed a saturation temperature decrease with pressure throughout the entire transient, decreasing to a value of 525 K at 30 s. The RELAP4 pretest prediction for the 0.457 m location coolant temperature indicated a quality of 1.0 would be reached at about 5 s into the transient.

The Critical Heat Flux Phenomena in the LLR Tests

Table III presents the measured times to departure from nucleate boiling and critical heat flux (CHF) for the LLR fuel rods based on thermocouple and LVDT readings. This table indicates the point at which the nucleate boiling heat flux rapidly decreased into a film boiling mode of heat transfer. At the point of critical heat flux, the steam formed a local insulating layer over the rod surface, resulting in a rapid increase in surface temperature. This blanket of vapor gradually propagated up (and possibly down) the fuel rod, starting at elevations apparently below the thermocouple locations. The range of incipient time to CHF at the thermocouple locations (near the axial location of peak power) for the 41- and 46 kW/m tests was from 1.8 to 2.6 s,

TABLE III MEASURED TIME (SECONDS) TO SATURATED DEPARTURE FROM NUCLEATE BOILING

Item	Test LLR-3	Test LLR-5	Test LLR-4	Test LLR-4A
Power (kW/m)	41	46	57	56
Rod 312-1				
TC 0° 0.533 m	2.40	1.80	1.65	
TC 180° 0.533 m	2.80	1.95	1.65	--
LVDT	2.80	0.5/1.5	0.25/1.5	
Rod 312-2				
TC 0° 0.457 m	2.60	2.00	1.60	1.85
TC 180° 0.533 m	4.50	2.3/3.3	1.95	2.10
LVDT	2.00	--	--	--
Rod 312-3				
TC 0° 0.533 m	2.50			
TC 180° 0.533 m	2.50	--	--	--
LVDT	2.00			
Rod 312-4				
TC 0° 0.533 m	2.40			
TC 180° 0.533 m	2.40	--	--	--
LVDT	1.80			
Rod 345-1				
TC 0° 0.533 m		1.8/3.9/4.7	1.65/4.0	2.0
TC 180° 0.533 m	--	1.9/3.9/5.0	1.65/3.65	2.0
LVDT		1.4/2.1/3.8	0.25/1.4/2.6	0.25/1.50
Rod 345-2				
LVDT	--	0.40	0.25	0.25/1.5/2.9
Rod 399-2				
TC 0° 0.314 m				1.60
TC 180° 0.457 m	--	--	--	1.75
LVDT				0.25/1.50/2.9

whereas the time of CHF in the 57- and 56 kW/m tests ranged from 1.6 to 2.0 s. The cladding elongation sensors (LVDTs) indicated that CHF occurred at an axial elevation below the surface thermcouples at about 0.25 s during the 57 and 56 kW/m tests and at about 0.4 to 0.5 s during the 46 kW/m test, excluding Rod 345-1.[a] The LVDT responses for the lowest power (41 kW/m test) ranged from 1.8 to 2.8 s. Since the LVDT detects CHF at any location along the length of the rod, and the surface thermocouples only indicate the time when the cladding at the thermocouple junction experiences CHF, the only time when the two measurements should be equal would be when the initial CHF condition occurs close to a thermocouple junction. Since the location of the thermocouples was originally chosen to correspond to the rod hot spots, and the LVDTs indicated CHF at 0.25 and 0.5 seconds rather than at 1.6 to 2.6 seconds, it is apparent that the surface thermocouples were delaying CHF in the upper portion of the fuel rods and at the axial elevation of peak power because of fin cooling; thus subsequently affecting the local temperature measurement.

The time to CHF for the RELAP4 pretest predictions was in the vicinity of 0.5 s. CHF was calculated to occur when the shroud flow rate decreased to a magnitude at which the code logic switched from the high flow saturated departure from nucleate boiling (DNB) correlation of Hsu and Beckner[2] to an interpolation between Hsu-Beckner and a modified Zuber[2] low flow CHF correlation. The Hsu-Beckner correlation is normally evaluated for mass fluxes greater than 1356 kg/m^2-s, whereas the modified Zuber correlation is applicable for mass fluxes less than 271. The calculated mass flux at the time of CHF was in the vicinity of 678. The actual expermental mass flux at 0.5 s could have ranged anywhere from 475 to 950. The RELAP4 heat transfer logic evaluates the local void fraction, and if it exceeds 0.96, dryout occurs. This dryout criteria arises from the Hsu-Beckner DNB correlation. The prediction of time to CHF is attributed to this code logic, since at 0.5 second, the hot spot quality was approximately 0.4, which resulted in a corresponding void fraction greater than 0.96.

---

a. Rod 345-1 behavior was influenced by a malfunctioning check valve above the rod which allowed upper plenum coolant to leak into the shroud flow channel, resulting in a premature quench for Tests LLR-5 and LLR-4A.

In a prior section it was postulated that an annular flow regime existed for the LLR flow shrouds for the first 6.5 to 7 s of the transients. The boiling crisis mechanism for the LLR tests was therefore probably an annular flow dryout, as suggested by Tong.[7] In this case, a liquid film covers and cools the heating surface. The boiling crisis occurs when the liquid film becomes too thin, and breaks into dry patches due to disruption of the annular liquid film from the high velocity vapor core. The characteristic of this crisis is a retarded wall-temperature excursion, which was evidenced in the LLR tests at the cladding surface thermocouple locations.

Test Rod Thermal and Mechanical Response

Selected fuel rod thermal-mechanical responses observed during each test are discussed in the following subsections. Some comparisons with pretest calculations are also shown. Table IV presents the maximum measured cladding temperature for each rod during each test. Although the data is limited, the measurements indicate that the peak cladding temperatures increased when the initial rod power was increased and were higher at lower axial elevations. The maximum temperature of 1260 K was attained at the 0.314 m location during the LLR-4A test. The RELAP4 pretest predictions indicated that the hot spot should have been at the 0.457 m elevation.

TABLE IV LLR FUEL ROD MAXIMUM MEASURED CLADDING TEMPERATURES

	Temperature (K)			
Rod	Test LLR-3	Test LLR-5	Test LLR-4	Test LLR-4A
312-1[a]	950	1000	1130	--
312-2[b]	925	1015	1170	1150
312-3[a]	1005	--	--	--
312-4[a]	870	--	--	--
345-1[a]	--	1005	1060	1075
345-2	Not instrumented with cladding thermocouples			
399-2[c]	--	--	--	1260

a. Measured at 0.533 m from bottom of heated length.
b. Measured at 0.457 m from bottom of heated length.
c. Measured at 0.314 m from bottom of heated length.

Test LLR-3. Test LLR-3 was conducted on February 28, 1979. The measured cladding temperatures for this test ranged from 870 to 1005 K. The measured cladding surface temperature, coolant temperature, cladding elongation, and the pretest calculated cladding surface temperature response of Rod 312-1 (a representative rod) during the first 20 seconds following initiation of blowdown are shown in Figure 15. The data indicates that the rod achieved DNB at 2.4 s and reached a maximum surface temperature of 950 K at 10 s. The LVDT response agrees favorably with the cladding temperature response, indicating CHF at 2.8 seconds. The underprediction in time to CHF by approximately 2.3 seconds by the RELAP4 code resulted in higher predicted cladding temperatures by as much as 140 K. On the basis of the maximum measured cladding temperature, no mechanical deformation is assumed to occurred to this rod during the LLR-3 test.

Test LLR-5. In keeping with the planned test sequence for LOFT, Test LLR-5 was conducted on March 24, 1979. The peak cladding temperatures ranged from 995 to 1015 K. Figure 16 shows the cladding surface temperature and cladding elongation responses for Rod 312-1. The maximum measured cladding surface temperature was 1000 K at the 0.533 m 0^{o} azimuthal thermocouple location, which indicated CHF at 1.8 s. The 0.533 m 180^{o} azimuthal cladding thermocouple indicated DNB at 1.95 s and a maximum cladding temperature of 990 K. The LVDT first indicated CHF at 0.5 second, with a second indication at 1.5 s. On the basis of measured cladding temperature and rod pressure comparisons with Olsen's data, no mechanical deformation is believed to have occurred at the thermocouple locations on any of the Test LLR-5 rods. However, subsequent cladding surface thermocouple evaluation tests have shown that surface thermocouples act as cooling fins, delaying CHF and reducing the peak cladding temperatures during a LOCA. The response of the LVDTs and cladding surface thermocouples during Test LLR-5 supports these conclusions. Apparently, the Test LLR-5 rods first reached CHF at an elevation below the thermocouples at 0.5 seconds and then reached CHF at the thermocouple junctions approximately 1.9 s, despite the fact that the thermocouples were located at the peak power elevation. This delay in time to CHF at the thermocouple junctions resulted in less stored energy at the time of CHF and measured temperatures possibly 60 K lower than at lower elevations. Therefore, the Test LLR-5 rods may have experienced buckling and incipient collapse.

Test LLR-4. Test LLR-4 was performed on March 30, 1979. Peak cladding temperatures of 1060 to 1170 K were measured, which resulted in significant mechanical deformation. Figure 17 shows the cladding temperature response for Rod 312-1. A cladding temperature of 1130 K was recorded at 7 s during the transient. The cladding thermocouples indicated the rod went into DNB at 1.65 s at both azimuthal locations, at the 0.533 m axial elevation. The LVDT for this rod first indicated CHF at 0.25 s with a second indication at 1.5 s. At approximately 15.4 seconds, the cladding surface thermocouples indicated quenching from the inadvertant loop isolation valve cycling. On the basis of comparisons with Olsen's data, the mechanical deformation of Rod 312-1 would be expected to include waisting (cladding collapse into pellet-to-pellet interfaces), as shown in Figure 18. Subsequent postirradiation examination (PIE) of Rod 312-1 confirmed this deformation.

As tabulated in Table III, the three operable LVDTs for this test first indicated DNB at 0.25 s at an axial elevation below the cladding surface thermocouple junctions (which were attached near the peak power elevation). Rods 312-1 and 345-1 subsequently had a second indication of CHF at 1.5 and 1.4 s, respectively, as CHF apparently propagated up the rod. The thermocouples for the rods indicated that CHF occurred at about 1.6 s. Thus, as in the prior tests, the external thermocouples influenced the fuel rod thermal response by delaying CHF and retarding the maximum cladding temperatures at the 0.533 m location and above. This delay in time to CHF reduced the measured temperatures at the 0.533 m location by an estimated 100 K. The RELAP4 pretest prediction of time to CHF for this test was approximately 0.5 s and the code overpredicted the cladding temperatures at the thermocouple locations by as much as 175 K. The RELAP4 calculated cladding surface temperatures at axial elevations slightly below the thermocouple junctions were probably only slightly above the actual temperatures.

Test LLR-4A. Since a major objective of performing the PBF/LLR Test Series was to evaluate the effect of cladding collapse and waisting on rod behavior during subsequent power ramps and depressurization transients, an additional LLR test, Test LLR-4A, was performed at the same test conditions as Test LLR-4. Rod 312-1 was removed prior to performing Test LLR-4A and

replaced with a fresh rod, designated 399-2. This permitted testing the mechanical deformation to be expected on a rod subjected to a single blowdown transient initiated from a power level of approximately 56 kW/m. During the power calibration and preconditioning power ramps, there were no observable indications that the deformed condition of the cladding on the other three test rods affected their behavior.

Peak cladding temperatures in the range of 1075 to 1260 K were measured during Test LLR-4A. As shown in Figure 19, the thermal and mechanical response of Rod 312-2 was essentially the same as that of Rod 312-1 during Test LLR-4 (Figure 17), with the rod achieving DNB at the 0.457 m thermocouple location at 1.85 s and reaching a maximum cladding temperature of 1150 K. Rod 399-2 reached the maximum measured cladding during the test, recording 1260 K at the 0.314 m thermocouple location.

The thermocouple effects evidenced in Test LLR-4A were similar to those witnessed in Test LLR-4. The LVDTs first indicated CHF at 0.25 s with a second indication at 1.5 s. The cladding surface thermocouples indicated CHF to first occur in the range of 1.6 to 2.0 s. This delay in time to CHF again probably reduced the measured temperatures at the 0.533 m location by as much as 100 K. The code underprediction of time to CHF, and the corresponding overprediction in cladding temperature at the thermocouple locations were comparable to the Test LLR-4 prediction.

No fuel rod failures were detected as a result of Test LLR-4A. Subsequent posttest examination of the rods revealed all four rods had achieved the waisting regime of mechanical deformation.

CONCLUSIONS

The PBF/LLR test program consisted of four sequential LOCA experiments during which seven PWR type fuel rods were evaluated. Measured cladding temperatures ranged from 870 to 1260 K when the rods were exposed to blowdown conditions similar to those expected in a PWR during a hypothesized double-ended cold leg break. The PBF/LLR Test Series fuel rods experienced the maximum mechanical deformation that would be expected to occur to the LOFT

fuel rods during the LOFT L2 Power Ascension Tests. The program demonstrated that low pressure, light water reactor design fuel rods, and specifically LOFT design fuel rods, are able to withstand successive preconditioning cycles and LOCA tests without failure.

Relative to the LLR tests themselves, several conclusions can be drawn. These include: (a) the mechanical deformation of the fuel rods that was observed during the postirradiation examination was consistent with Olsen's criteria for fuel rod deformation; (b) thermocouple and LVDT behavior indicated DNB was first observed at an elevation lower than the peak power elevation; (c) the lower elevations consequently achieved higher cladding temperatures; (d) the delay in CHF and lower cladding temperatures at the peak power elevation is attributed to a fin cooling effect caused by the geometry of the cladding surface thermocouples; and (e) the RELAP4 code accurately predicted the system thermal-hydraulic behavior, but underpredicted times to CHF, and subsequently predicted higher cladding temperatures than measured at the thermocouple locations. However, the RELAP4 cladding temperature predictions may be close to the actual temperatures at locations without thermocouple attachments.

ACKNOWLEDGEMENTS

The authors express their appreciation to R. K. McCardell and D. R. Evans for their assistance in this study.

REFERENCES

1. D. L. Reeder, LOFT System and Test Description, NUREG/CR-0247, TREE-1208 (July 1978).

2. K. R. Katsma et al., RELAP4/MOD5-A Computer Program for Transient Thermal-Hydraulic Analysis of Nuclear Reactors and Related Systems, NUREG-1335 (September 1976).

3. J. R. Larson, PBF-LOCA Test Series Test LOC-11 Test Results Report, NUREG/CR-0618, TREE-1329 (April 1979).

4. C. S. Olsen, "Zircaloy Cladding Collapse Under Off-Normal Temperature and Pressure Conditions," NUREG-1239 (April 1978).

5. J. G. Collier, Convective Boiling and Condensation, McGraw-Hill, 1972.

6. G. F. Hewitt, and D. N. Roberts, Studies of Two-Phase Flow Patterns by Simultaneous X-Ray and Flash Photography, AERE-M 2159, (1969).

7. L. S. Tong, Boiling Crisis and Critical Heat Flux, AEC Critical Review Series (August 1972).

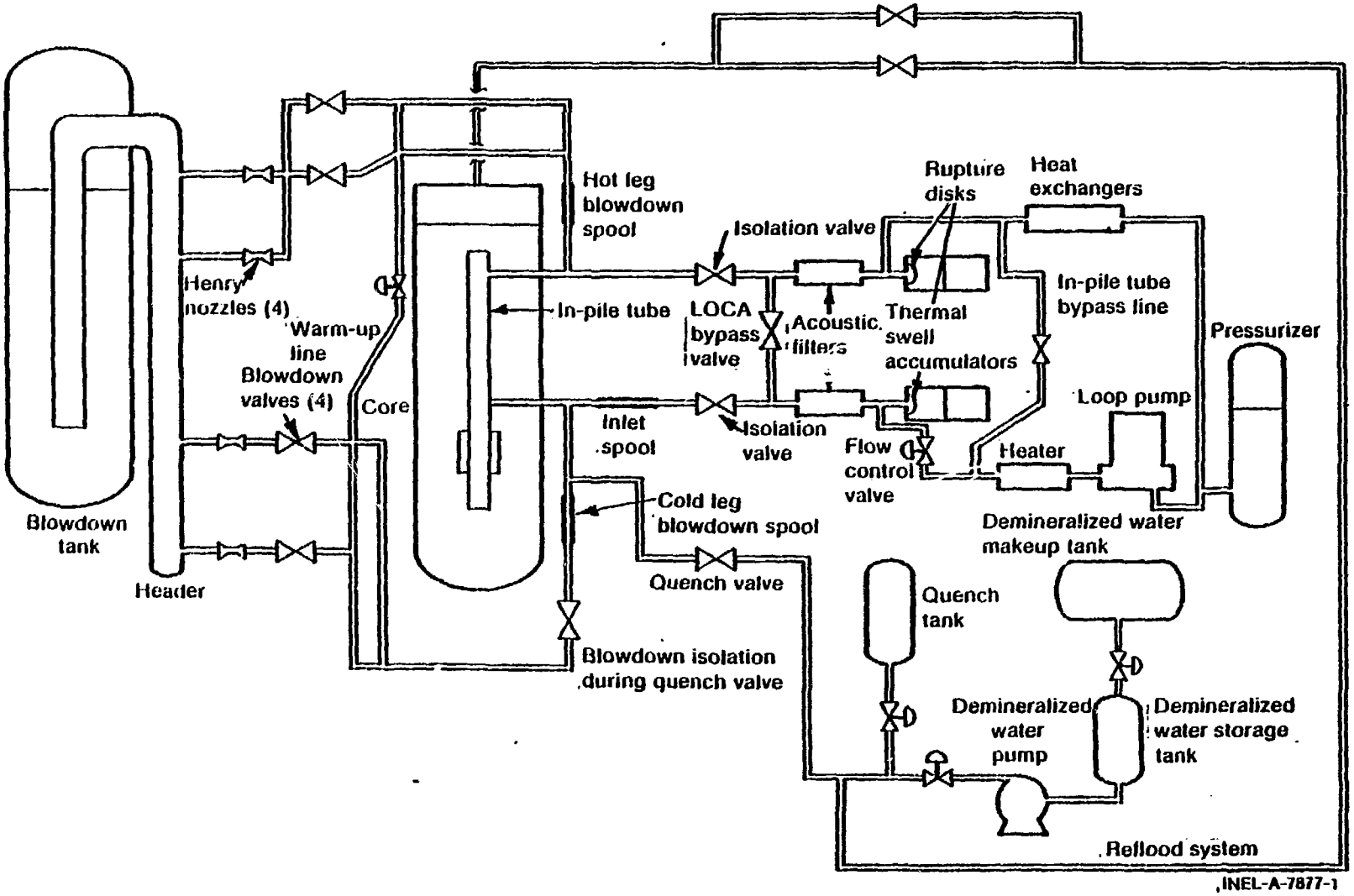

Fig. 1 PBF/LOCA blowdown loop.

PBF Inpile Tube and LLR Test Train

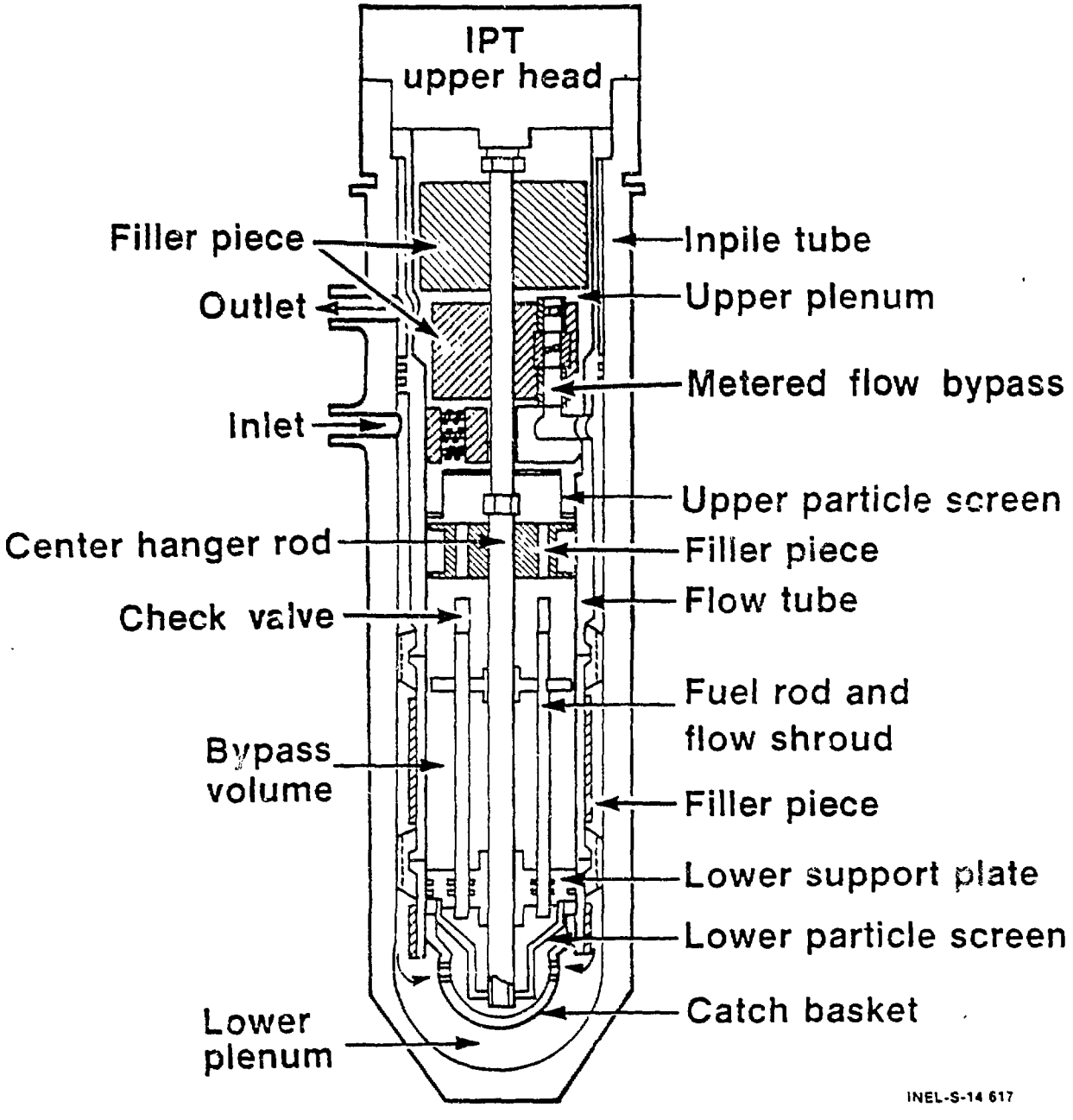

Fig. 1a PBF In-Pile Tube and LLR Test Train.

Test Configuration Schematic

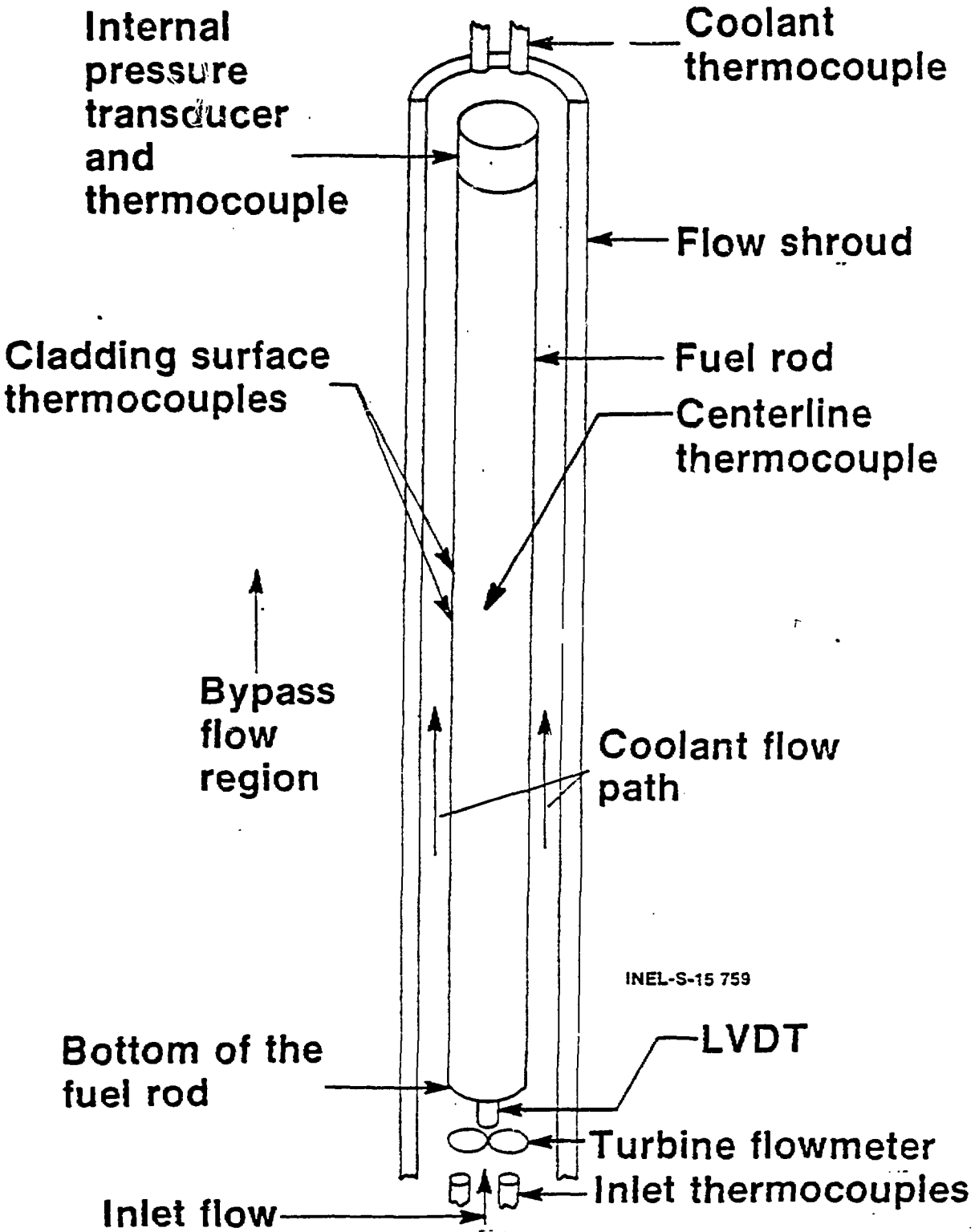

Fig. 2 PBF/LLR test configuration schematic.

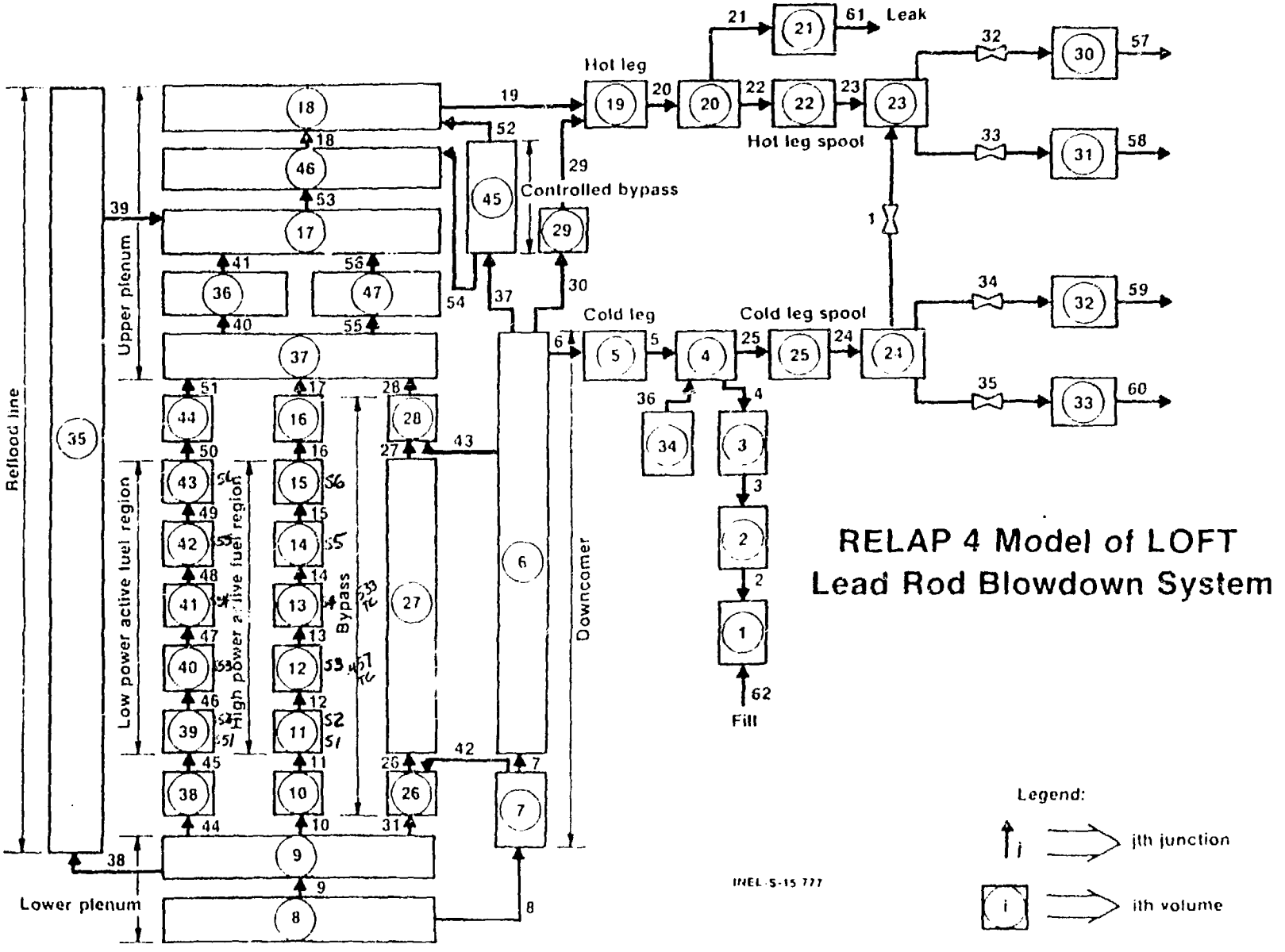

Fig. 3 RELAP 4 model of LOFT lead rod blowdown system.

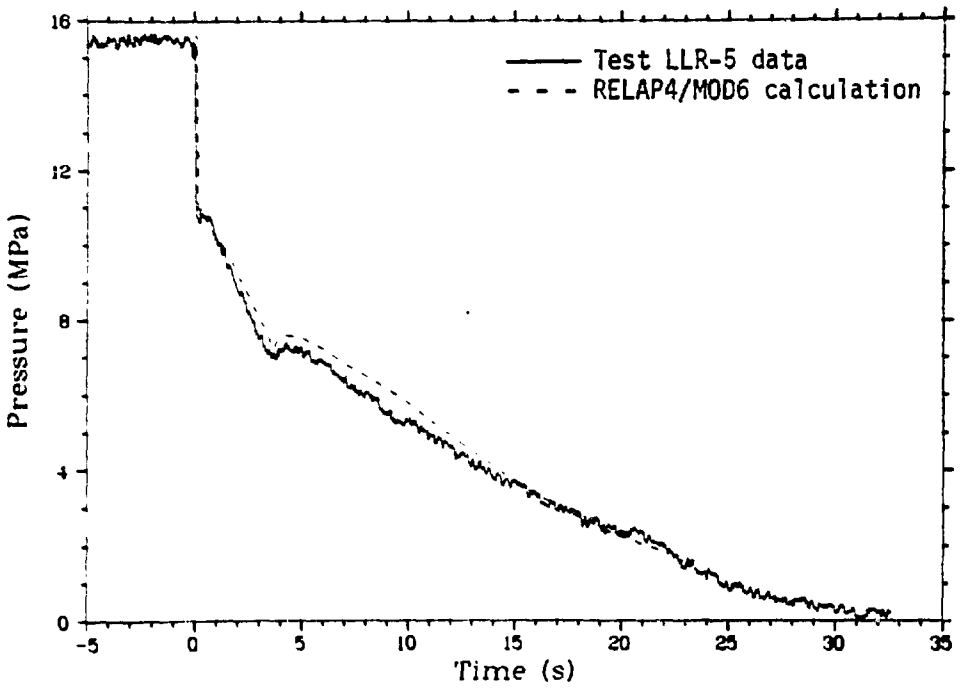

Fig. 4 Comparison of calculated and measured system depressurization in cold leg blowdown spool during Test LLR-5.

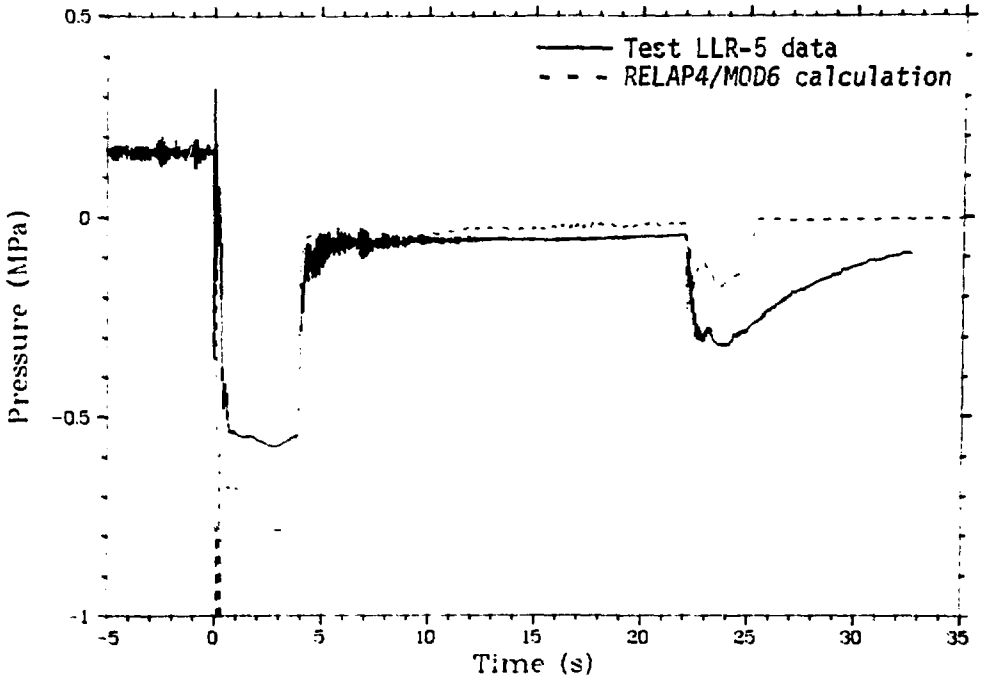

Fig. 5 Comparison of calculated and measured cold to hot leg differential pressure during Test LLR-5.

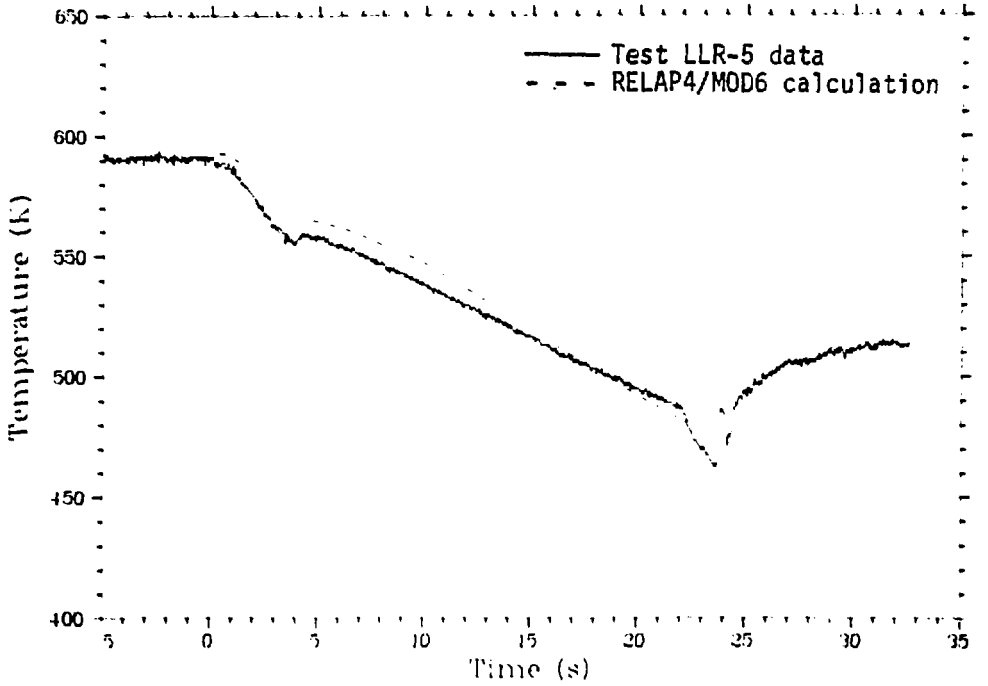

Fig. 6 Comparison of calculated and measured coolant temperature in cold leg spool during Test LLR-5.

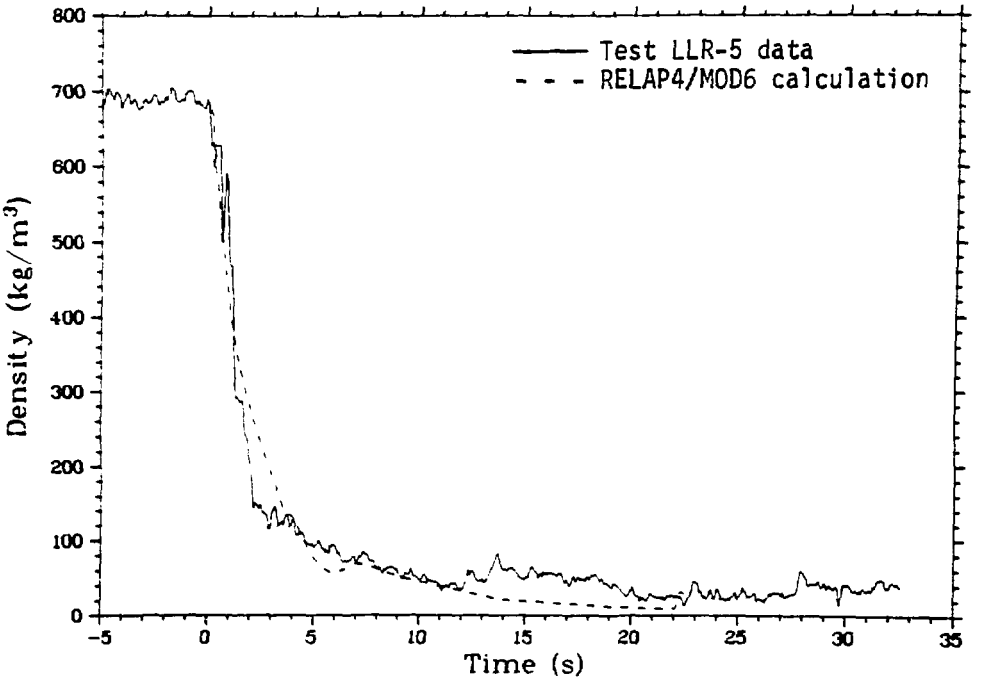

Fig. 7 Comparison of calculated and measured coolant density in cold leg spool during Test LLR-5.

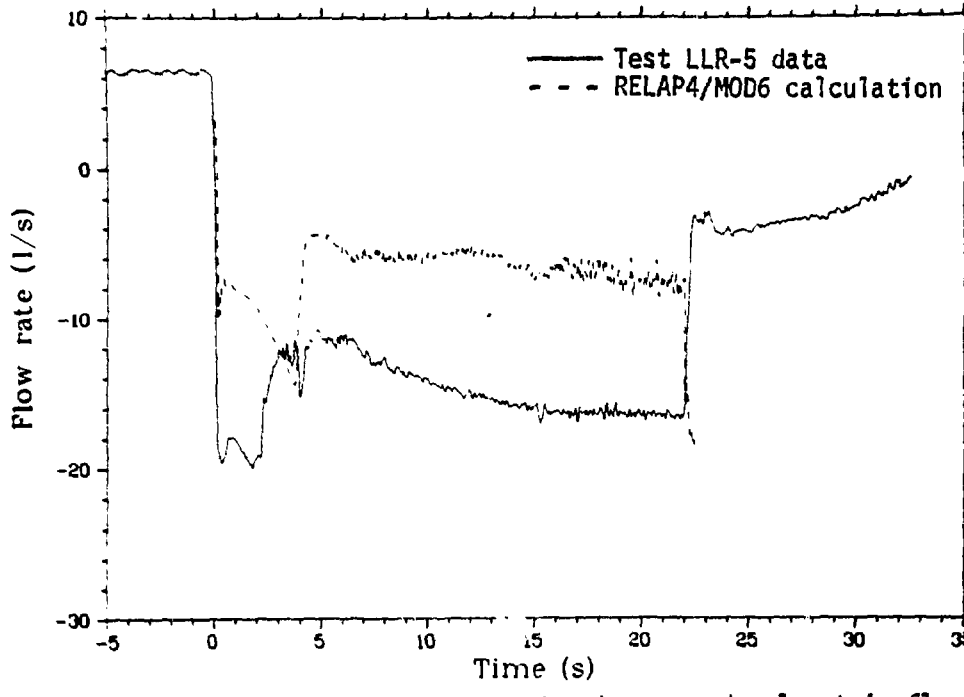

Fig. 8 Comparison of calculated and measured volumetric flow rate in the controlled bypass.

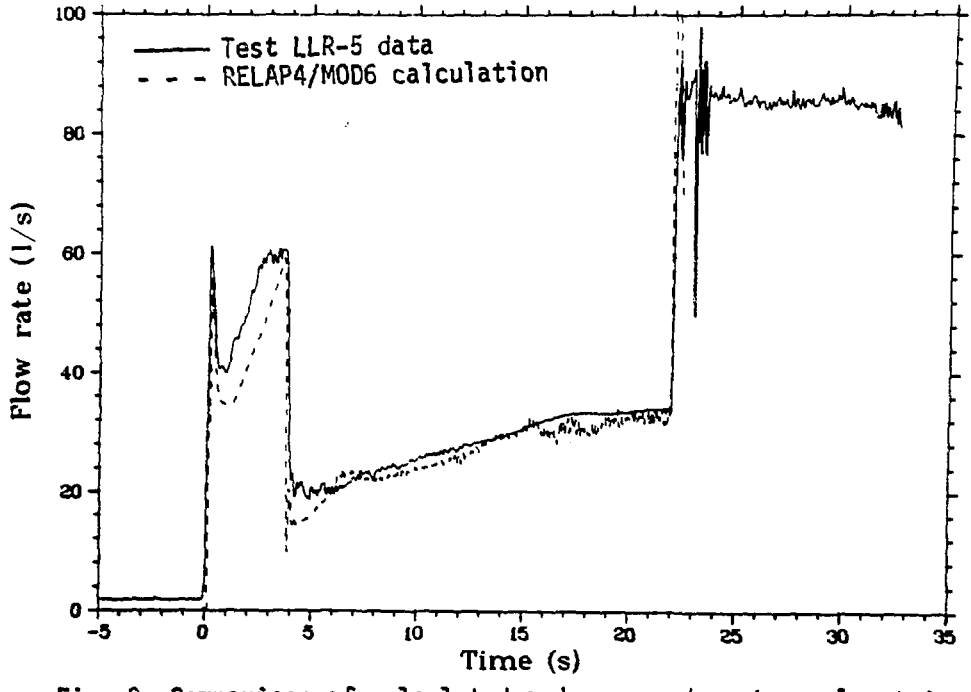

Fig. 9 Comparison of calculated and measured system volumetric flow in cold leg spool during Test LLR-5.

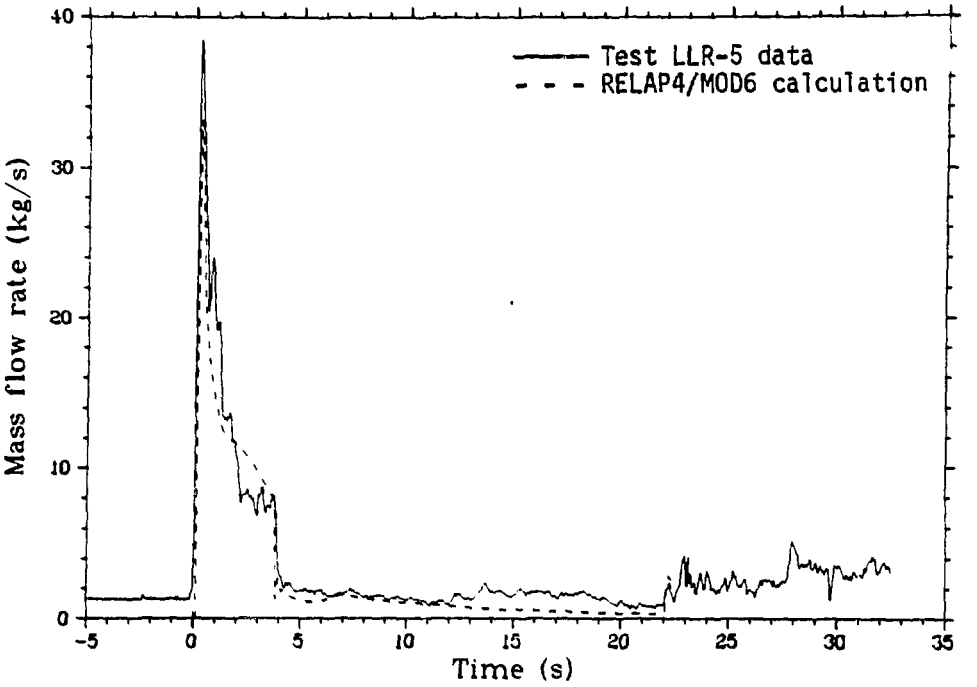

Fig. 10 Comparison of calculated and measured mass flow in cold leg spool during Test LLR-5.

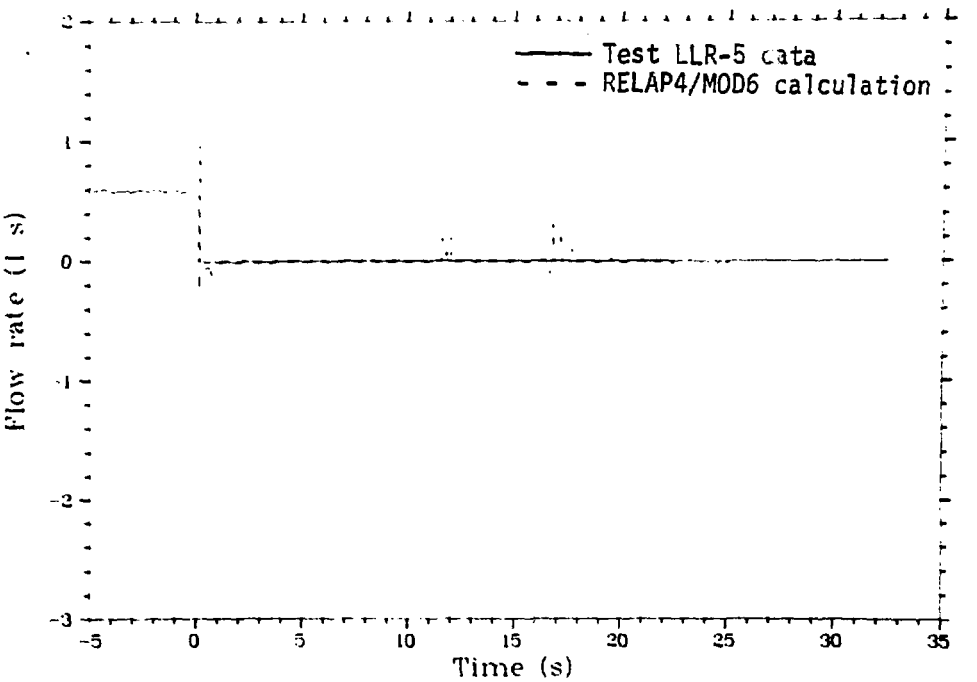

Fig. 11 Comparison of calculated and measured upper turbine volumetric flow rate during Test LLR-5.

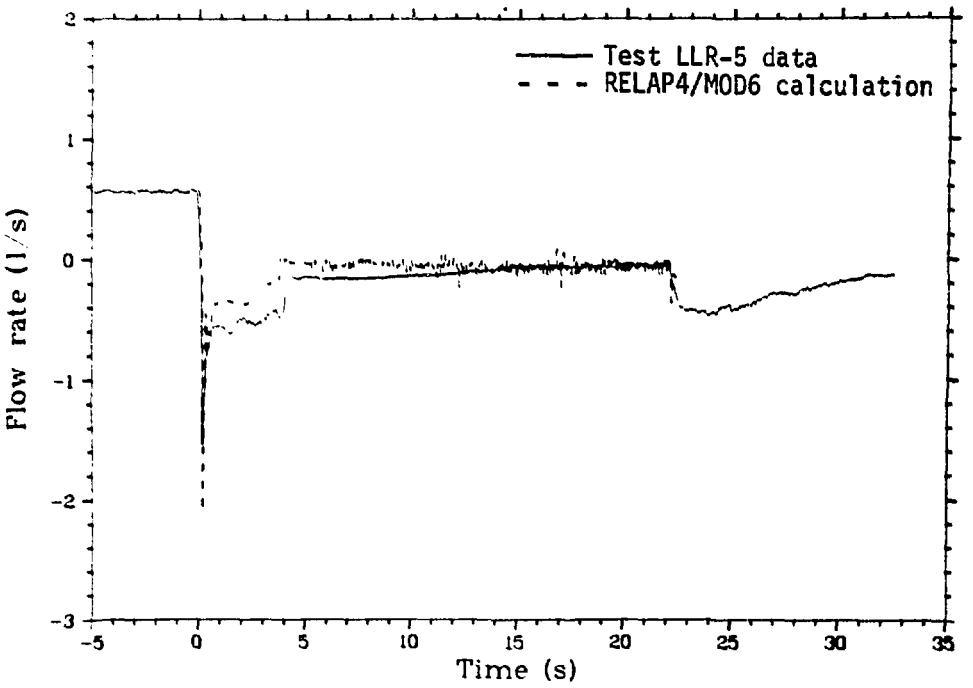

Fig. 12 Comparison of calculated and measured lower turbine volumetric flow rate during Test LLR-5.

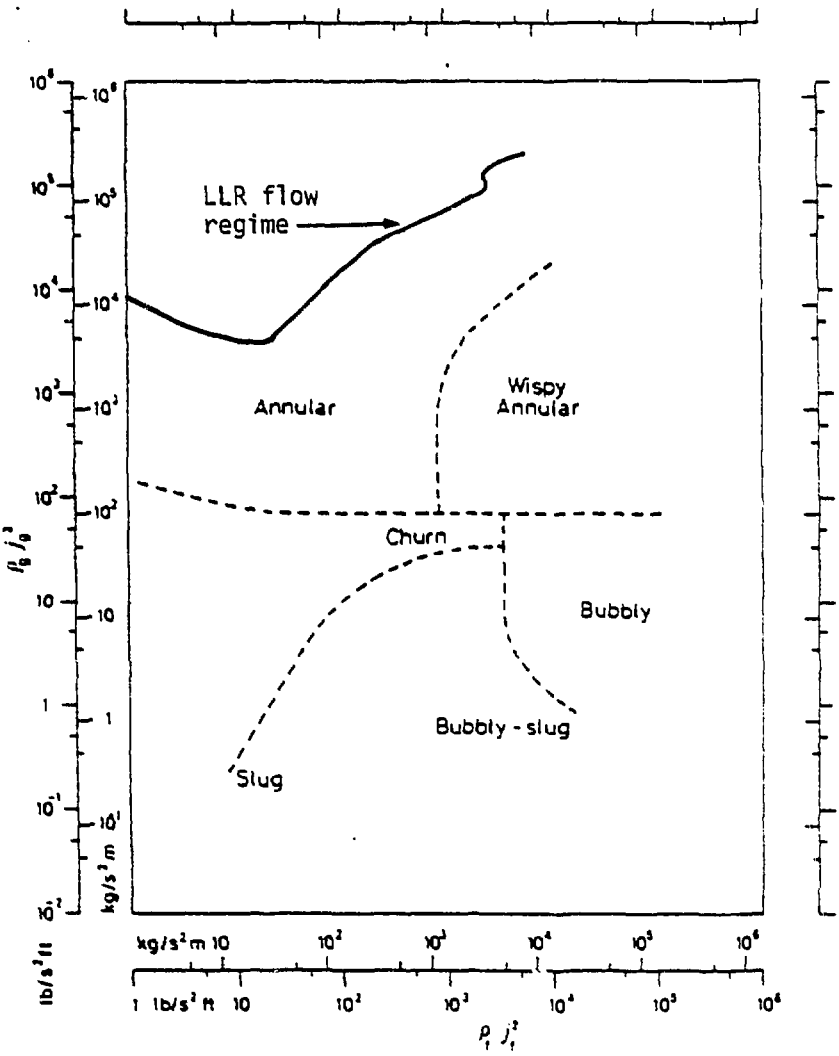

Fig. 13 Flow pattern map for vertical flow in LLR flow shrouds during LLR-5.

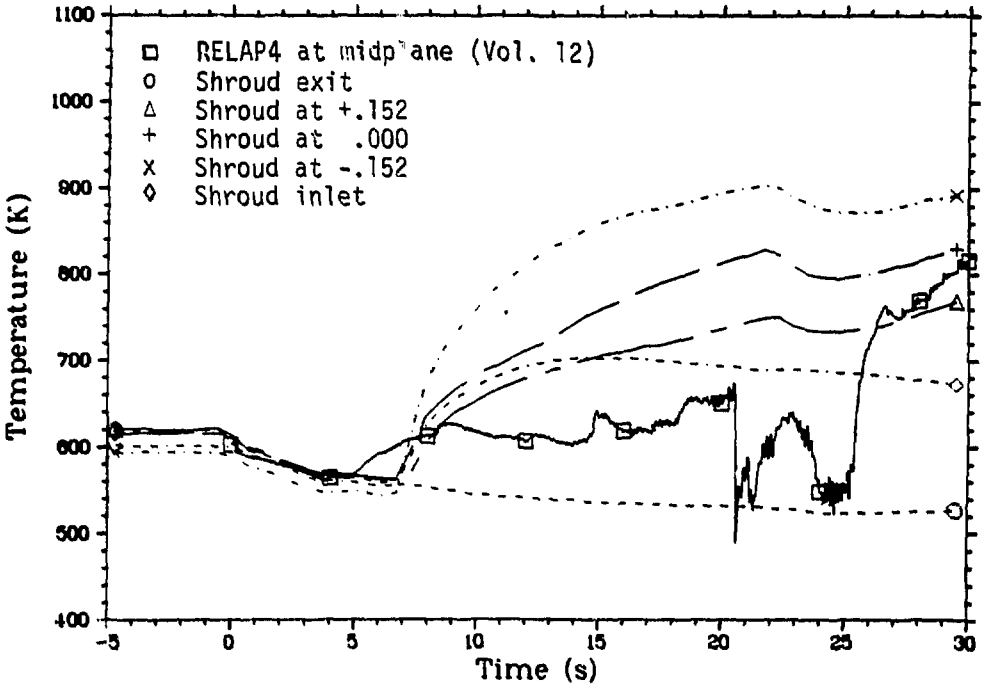

Fig. 14 Coolant temperatures in shroud 345-1 for Test LLR-5.

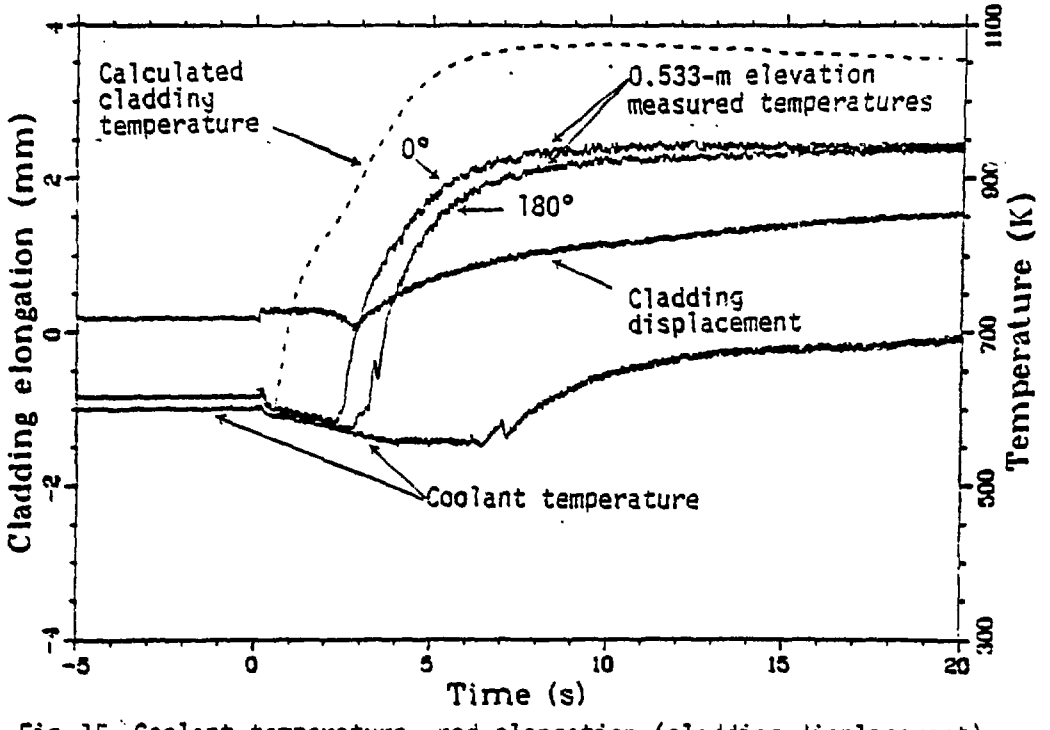

Fig. 15 Coolant temperature, rod elongation (cladding displacement), and calculated and measured cladding temperature for Rod 312-1 during Test LLR-3.